helpful discussions, to J. R. Hill, 3M Analytical and Properties Research Laboratory, for obtaining many of the NMR spectra; to T. Kestner for the 2.3-T ^{195}Pt spectra, and to R. J. Koshar, 3M Industrial and Consumer Sector Laboratory, for gifts of the fluorocarbon acids. Our understanding of the kinetics of platinum dimer formation was facilitated by Dr. G. V. D. Tiers and the helpful comments of a referee.

Supplementary Material Available: Tables of positional and thermal parameters, hydrogen positional parameters, anion and solvent bond lengths, general temperature factor expressions, root-mean-square amplitudes of thermal vibrations, cation bond lengths and angles, torsional angles, least-squares planes, and observed and calculated structure factors (53 pages). Ordering information is given on any current masthead page.

Infrared Photochemistry of Oxetanes: Mechanism of Chemiluminescence

William E. Farneth*[†] and Douglas G. Johnson[‡]

Contribution from the Department of Chemistry, University of Minnesota, Minneapolis, Minnesota 55455, E. I. du Pont de Nemours and Company, Central Research and Development Department, Experimental Station 356/231, Wilmington, Delaware 19898, and Department of Chemistry, University of Chicago, Chicago, Illinois 60637. *Received May 8, 1985*

Abstract: The infrared multiphoton (IRMP) induced photolysis of several oxetanes is examined at low pressures (ca. 100 mtorr) while experimental variables such as laser frequency, laser energy, bath gas, and bath gas pressure are altered. The products of the IRMP induced photolysis of 2-acyl-3-ethoxy-2-methyloxetane, Ox1, are primarily biacetyl and ethyl vinyl ether. When the photolysis is run with the collimated beam of a CO_2 laser (1-3 J/cm^2) luminescence is observed. The intensity of the luminescence varies with the efficiency of the unimolecular decomposition of the oxetane. On the basis of the spectral distribution and temporal behavior of the luminescence following irradiation of Ox1, the emitter is believed to be vibrationally hot electronically excited biacetyl. Similar experiments with 2,2-dimethyl-3-ethoxyoxetane give a weaker emission apparently due to excited-state acetone. Results are discussed in terms of the reverse of the Paterno-Buchi reaction—a diabatic retrophotocycloaddition.

Conventional photochemistry involves a surface crossing at some point along the reaction coordinate. The location of the surface crossing relative to the amount of nuclear reorganization that has occurred has been used to categorize photochemical reactions as "adiabatic" or "diabatic"[1]. Those photochemical reactions where the surface crossing is either the first event following photoexcitation ("hot ground-state reactions") or the last event following all changes in bonding ("chemiluminescent reactions") are termed adiabatic since nuclear reorganization takes place completely on one surface. Those photochemical transformations which return to the ground electronic surface somewhere along the reaction coordinate are referred to as diabatic. Most photochemical reactions are believed to be diabatic.

Infrared multiphoton induced photochemistry is different. Most IRMP induced reactions are adiabatic. Excitation and reaction are usually confined to the ground electronic surface. IRMP induced chemiluminescent reactions are the exception. A number of chemiluminescent processes have been reported. However, these require high laser powers and most involve extensive fragmentation of the reactants to open-shell species.[2-5] One example which appears to give closed-shell species is the IRMP induced decomposition of tetramethyldioxetane (TMD) to yield excited-state acetone.[2] In this case the IRMP induced diabatic chemistry mimics the known thermal chemistry since chemiluminescence in the pyrolysis of TMD is a well-established phenomenon.[6]

We thought it should be possible to extend the observation of IRMP induced chemiluminescence to systems where chemiluminescence had not been observed following thermal excitation. We were particularly interested in systems where the ground-state-to-excited-state surface crossing required for IRMP induced chemiluminescence would constitute the reverse of the excited-state-to-ground-state crossing in a known diabatic conventional photochemical reaction. The photoaddition of ketones and olefins to form oxetanes appeared to be an attractive system for study.[7,8] We have chosen to concentrate on 2-methyl-2-acyl-substituted oxetanes since biacetyl (lowest excited state of about 57 kcal/mol[9]) would be an expected carbonyl fragment in the decomposition. These oxetanes can be made by the addition of photoexcited biacetyl to vinyl ethers.[10] Thus, an IRMP induced diabatic retro-2 + 2-photocycloaddition (evidenced by photon emission from the product) would be the formal reverse of a known diabatic 2 + 2-photocycloaddition.

The IRMP induced photochemistry of three oxetanes, 2-acyl-3-ethoxy-2-methyloxetane (Ox1), 2,2-dimethyl-3-ethoxyoxetane (Ox2), and 2-acyl-2,3-dimethyl-3-methoxyoxetane (Ox3), was studied in some detail. In each case the major products were determined, and the rates (overall) of oxetane loss during pulsed irradiation were measured under various conditions. Ox1 was the most thoroughly examined system. Luminescence has been observed.

Experimental Section

The excitation source used was a pulsed (0.5 Hz), grating turned CO_2 (TEA) laser. The pulse shape, under typical experimental conditions, consisted of an initial spike (250 ns FWHM) followed by a tail out to 1.2 μs. The initial spike delivered 90% of the total pulse energy.

[†] E. I. du Pont de Nemours and Company.
[‡] University of Chicago.

(1) (a) Forster, Th. *Pure Appl. Chem.* **1973**, *34*, 225. (b) Michl, J. *Pure Appl. Chem.* **1975**, *41*, 507.
(2) Yahav, G.; Haas, Y. *Chem. Phys.* **1978**, *35*, 41-49.
(3) Farneth, W. E.; Flynn, G.; Slater, R.; Turro, N. J. *J. Am. Chem. Soc.* **1976**, *98*, 7877.
(4) Watson, T. A.; Mangir, M.; Wittig, C. *J. Chem. Phys.* **1981**, *75*, 5311-5317.
(5) Ambartzumian, R. V.; Chekalin, N. V.; Letokhov, V. S.; Ryabov, E. A. *Chem. Phys. Lett.* **1975**, 36, 301.
(6) Turro, N. J.; Lechtken, P.; Schore, N. E.; Schuster, G.; Steinmetzer, H. C.; Yekta, A. *Acc. Chem. Res.* **1974**, *7*, 97.
(7) Johnson, D. G. Ph.D. Thesis, University of Minnesota, 1985.
(8) Farneth, W. E.; Johnson, D. G. *J. Am. Chem. Soc.* **1984**, *106*, 1875.
(9) Turro, N. J. "Modern Molecular Photochemistry"; Benjamin/Cummings: London, 1978, p 116.
(10) Jones, G., II; Santhanam, M.; Chiang, S. *J. Am. Chem. Soc.* **1980**, *102*, 6077.

0002-7863/86/1508-0773$01.50/0

The frequency of the output was determined with an Optical Engineering 16A spectrum analyzer. Laser power and energy were measured with a volume absorbing calorimeter (Scientech, model #380 102). Typical pulse energies ranged from 0.1–0.5 J/pulse. The temporal profile of the output was measured with a photon drag detector (Rolin, model #7400). The spatial profile of the beam was determined by the image formed on thermal-sensitive paper. The cross section of the beam was approximately circular in shape with a diameter of 1.4 cm. Unless otherwise stated all experiments reported were performed with a collimated beam. The initial laser output was sent consecutively through zinc selenide lenses of 15 in. and 5 in. focal lengths aligned 20 in. apart. This telescoping arrangement gave typical fluences of 1–3 J/cm^2.[11] Collimation produces a cylindrical reaction volume through the entire length of the cell. Since the beam is insignificantly attenuated along the cell length the fluence is essentially uniform throughout the reaction volume. When necessary the beam was attenuated with either NaCl plates or sheets of polyethylene film.

The oxetanes were loaded into cylindrical Pyrex cells from a mercury free vacuum line. The cells (3 in. length and 1 in. diameter) were designed with various ports governed by Teflon stopcocks. The ends of the cells were fitted with NaCl or KCl windows. The gas cells used for emission experiments were crosses made from Pyrex tubing. The typical cell was 23 cm long (1.6 cm i.d.) crossed perpendicularly in the center by a section 5 cm long (4.3 cm i.d.). The longer section was fitted with NaCl windows, front and rear, while the 5-cm section was fitted with Pyrex windows. The PMT viewed the reaction region through Pyrex windows. Experiments were typically run with oxetane pressures in the range of 100 mtorr. Pressures were measured with a capacitance manometer (Baratron Model 227).

The collimated beam from the CO_2 laser was sent through a germanium window into a light-tight enclosure. The enclosure contained an optical rail on which the reaction cells and the calorimeter were mounted. Within this region a photomultiplier tube (EMI PMT #9635B) was mounted perpendicular to the cell. The signal from the PMT was sent via a preamp to a Biomation 8100 waveform recorder. Most of the relevant data were recorded with sample intervals of either 0.01 or 0.05 μs. The total time of data collection was 20 or 104 μs, respectively. A small portion of the laser beam was split out by a NaCl plate and sent to a pyroelectric detector. This signal was used to trigger the waveform recorder and to correct for pulse-to-pulse fluctuations in laser power.

Infrared spectra were obtained on a Beckman 4250 infrared spectrometer. Fourier transform infrared spectra were taken with a Digilab FTS-10 spectrometer. Gas chromatographic analyses of reaction mixtures following irradiation were accomplished with direct injection of the gas samples onto the column of either a Varian 2400 or 1200 $^1/_8$-in. column gas chromatograph. The following $^1/_8$-in. GC columns were used in the analysis of the photolysis mixtures: column 1, 20 ft 10% UCON LB550-X; column 2, 10 ft 10% UCON LB550-X; column 3, 19 ft 10% QF-1. All liquid phases were supported by AWDMSC-Chromosorb-W.

All three oxetanes—Ox1, Ox2, and Ox3—were prepared by Paterno–Buchi reactions of the appropriate ketone and the corresponding enol ether: Ox1—Biacetyl, ethyl vinyl ether,[12] Ox2—acetone, ethyl vinyl ether,[13] and Ox3—biacetyl, 2-methoxypropene.[12] All three oxetanes were purified by preparative gas chromatography prior to use.

Results

Two categories of experiments will be described: (1) those which characterize the photochemistry and (2) those which characterize the IRMP-induced emission. The former experiments include identifying products, measuring the efficiency of reaction, and determining the nature of the excitation process. The latter experiments address the identity of the emitter(s), the characteristics of the emission, and the effect of several parameters on the efficiency of emission.

IRMP Photolysis. The identities of the major products of the IRMP photolysis of Ox1, Ox2, and Ox3, were determined by using gas chromatography and IR analysis. From each oxetane there were two main products. The IRMP-induced decomposition of Ox1 yielded a reaction mixture showing three product peaks, [1A], [1B], and [1C], by GC analysis (column 2). These peaks (uncorrected) accounted for 2% (±0.5%), 64.0% (±1%), and 33.5% (±1%), respectively, of the total product integral. Coinjection of biacetyl and ethyl vinyl ether on both column 2 and column 3 showed product peak [1B] to be ethyl vinyl ether and [1C] to be biacetyl. Peak [1A] (2% of product mixture) was not specifically identified. Its retention time was consistent with a very low boiling hydrocarbon such as ethane, ethylene, or methane.

GC analysis of the photolysis mixture of Ox1 showed no peaks which could be attributed to products of the alternative retro 2 + 2 fragmentation pattern. Such products from Ox1 would be 4-ethoxy-2-methyl-3-buten-2-one and formaldehyde. Neither of these compounds is particularly amenable to gas-phase injection. However, no evidence for these products was observed by direct gas injection or following condensation of the contents of the reaction cell into a trap at −196 °C and GC analysis of the condensate. The products of the IRMP photolysis of Ox1 have also been examined by FTIR spectroscopy. The IR difference spectrum, obtained by subtracting the spectrum of Ox1 from the spectrum of the photolysis mixture following 600 pulses, has been previously reported.[8] This subtraction spectrum can be completely accounted for by summing the IR spectra of ethyl vinyl ether and biacetyl. The FTIR experiments gave no positive indication of formaldehyde.[14]

Gas chromatographic analysis (column 1; temperature program 15–80 °C begining at time equals 2 min at 8 °C/min) of the reaction mixture following IRMP-induced decomposition of Ox2 again showed three main product peaks, [2A], [2B], and [2C]. The second two peaks, [2B] and [2C], accounted for 95% (uncorrected) of the total integrated area. Coinjection experiments using columns 1, 2, and 3 showed peaks [2B] and [2C] to have retention times identical with ethyl vinyl ether and acetone, respectively. No peak was enhanced when acetaldehyde was coinjected. The minor product peak, [2A], accounted for 4.8% (uncorrected) of the observed products. The retention time of [2A] was barely resolved from the air peak on column 1.

IRMP-induced decomposition of Ox3 yielded two major peaks. Coinjection on columns 1 and 3 gave retention times consistent with biacetyl and 2-methoxypropene. These experiments were conducted at various fluences such that the conversion in 100 pulses varied from 5% to 20%. In all cases GC analysis of the resulting reaction mixtures detected only biacetyl, 2-methoxy propene, and Ox3.

While qualitative GC analysis of the products was possible, quantitative analysis of the reaction mixture was complicated by the low vapor pressures of the oxetanes and adsorption of Ox1, Ox3, and biacetyl on O-rings and stopcock surfaces. It was difficult to establish percent conversions by GC because the amount of unconverted Ox1 could not be accurately determined. Relative amounts of ethyl vinyl ether (EVE) and biacetyl could be reasonably estimated for samples which were measured under rigorously identical conditions. Experimental product ratios were calibrated by using mixtures of known pressures of EVE and BA. The control experiments showed that these ratios were sensitive to loading techniques, sample age, pump efficiency, and some undetermined variables. Nevertheless, when carefully monitored, sufficient reproducibility was obtained. The ratio of EVE to biacetyl calibrated in this way was 0.96 (±0.10).

A rate constant for decomposition over a number of pulses (k_{rxn} pulse^{-1}) was used to quantify the efficiency of the reaction. Values of k_{rxn} were obtained by fitting the increase in pressure during photolysis to an exponential growth curve. The fit assumed that each molecule decomposed to two product molecules and that no secondary decomposition took place—either immediately or in later pulses. This is the reaction course suggested by the product distributions described earlier. These assumptions were further justified by the following observations: (1) GC analysis of the cell contents following irradiation at 967.72 cm^{-1} of either biacetyl or EVE showed no reaction products. (2) There was no appre-

(11) It is important to note the nature of the laser beam in comparing IRMP experiments. Most luminescence experiments employ focused geometries where focal point fluences may reach values greater than 100 J/cm^2, e.g., ref 22. The telescoped, collimated beam arrangement employed in these experiments constitutes a spatially more homogeneous and energetically less intense arrangement.

(12) Ryang, H. S.; Shima, K.; Sakurai, H. *J. Org. Chem.* **1973**, *38*, 2860.

(13) Schroeter, S. H.; Orlando, C. M., Jr. *J. Org. Chem.* **1969**, *34*, 1181.

(14) Herzberg, G. "Electronic Spectra and Electronic Structure of Polyatomic Molecules"; Van Nostrand: New York, 1966 (no 1746 cm^{-1} peak observed).

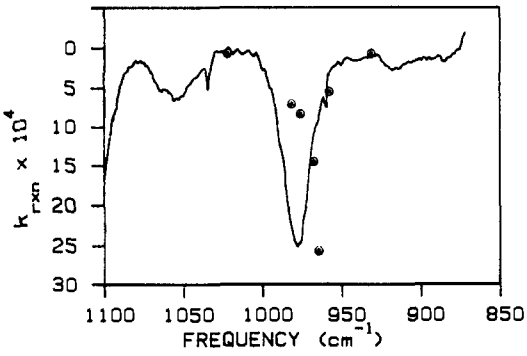

Figure 1. IR action spectrum of Ox1 (k_{rxn}) (symbols) superimposed on the single photon absorption spectrum of Ox1 (solid line).

Table I. The Effect of Fluence on Reaction Efficiency and Peak Emission Intensity

		k_{rxn}, pulse^{-1}	
fluence, J/cm^2	lum. int., au	measd	calcd[a]
1.29	7	1.6×10^{-4}	1.6×10^{-4}
1.35	17		2.4×10^{-4}
1.41	21		3.3×10^{-4}
1.44		3.5×10^{-4}	3.8×10^{-4}
1.47	40		4.4×10^{-4}
1.53	60		6.0×10^{-4}
1.59	102		8.0×10^{-4}
1.62	117		9.4×10^{-4}
1.68		16×10^{-4}	13×10^{-4}
1.82		32×10^{-4}	26×10^{-4}
2.00		48×10^{-4}	63×10^{-4}

[a] Calculated k_{rxn} values are interpolations of the line $\ln(k_{rxn})$ vs. fluence ($r = 0.991$).

ciable pressure increase during photolyses of either biacetyl or EVE. The k_{rxn} values obtained were not entirely independent of the extent of reaction. As the reaction proceeds the pressure in the reaction cell increases and collisional quenching causes k_{rxn} to fall. However, when k_{rxn} was determined for the first 12–15% of reaction, the correlation coefficients were ≥0.995. The linearity of the expontential fit shows that each pulse may be treated as an individual experiment over this conversion range. That is, what occurs during a 200-pulse photolysis is essentially the sum of 200 single pulse experiments. The time between pulses was much greater than the effective reaction time.

The response of the IR photochemistry of oxetanes to changes in fluence, irradiation frequency, and bath gas is quite similar to what has been observed with other large molecules.[15,17] The magnitude of k_{rxn} varied with the wavelength of irradiation. Figure 1 shows a rough IR action spectrum of Ox1 superimposed on the single photon absorption spectrum of Ox1. The action spectrum maximum appears some 10–15 cm^{-1} to the red of the single photon absorption maximum. This type of red shift is common in the action spectrum of IRMP induced processes.[15,18]

With other parameters constant (100 mtorr Ox1, 967.72 cm^{-1}) the reaction is sensitive to the power of the laser pulse. Efficiency of conversions varied from $k_{rxn} < 0.5 \times 10^{-4}$ pulse^{-1} at 0.78 J/cm^2 to $k_{rxn} = 48.0 \times 10^{-4}$ pulse^{-1} at a fluence of 2.00 J/cm^2 (Table I). Added argon pressures from 300 mtorr to 2.0 torr caused k_{rxn} of Ox1 to drop by well over an order of magnitude.

An important question to answer about any IRMP-induced photolysis is whether the energy acquisition for reaction is photon absorption (nonthermal) or collisional activation (thermal). A common characteristic of IRMP-induced, nonthermal processes is the selective destruction of an absorbing species in the presence of a nonabsorbing species of similar thermal reactivity.[15] "Chemical thermometer" experiments of this kind were performed with Ox1 and 4-vinylcyclohexene (VCH). 4-Vinylcyclohexene was chosen for these mixed-gas experiments for three reasons: (1) VCH is effectively transparent at the frequency used to induce Ox1 decomposition (967.72 cm^{-1}). (2) VCH has a strong absorption feature within the range available to the CO_2 laser where Ox1 is transparent. (3) VCH undergoes a retro-Diels–Alder reaction (yielding butadiene) with Arrhenius parameters similar to those estimated for Ox1 (A factor ca. $10^{15.2}$; E_a ca. 62 kcal/mol[16]).

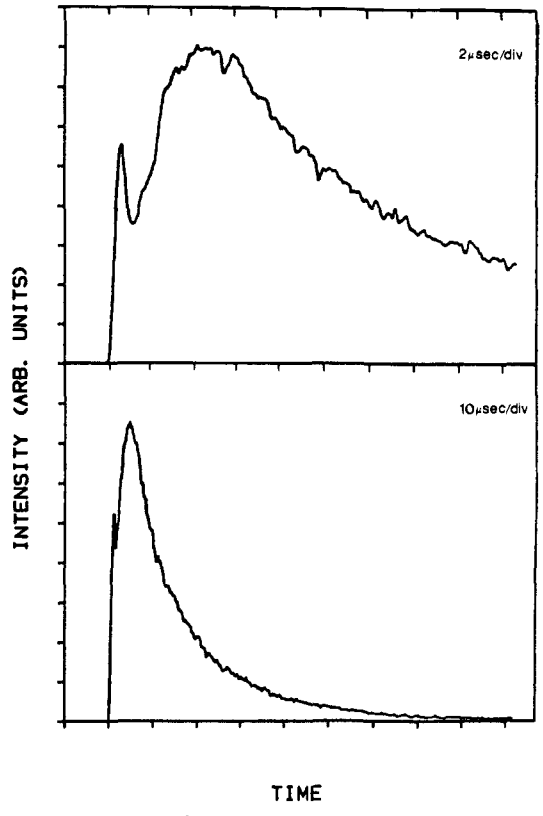

Figure 2. Total emission from a 100-mtorr sample of Ox1. Upper: 2.0 μs per division. Lower: 10.0 μs per division.

Samples (100 mtorr) of VCH were irradiated (967.72 cm^{-1}) with powers of 0.44 and 0.80 J/pulse for 250 pulses by using a collimated beam arrangement. GC analysis (column 1) of the reaction mixtures showed neither butadiene nor any other product peaks at either fluence. When the pressure within the reaction cell was monitored, no pressure increases were observed. This demonstrated that there was no direct excitation of VCH under typical Ox1 reaction conditions. However, irradiation at 916.7 cm^{-1}, where VCH is a relatively strong absorber, produced observable decomposition.

Mixtures of 50-mtorr VCH and 100-mtorr Ox1 were irradiated at a frequency of 967.72 cm^{-1} and a pulse energy of 0.46 J for 500 pulses. GC analysis showed no detectable quantity of butadiene while EVE and biacetyl were both detected. During photolysis the pressure changed from 146 mtorr (50-mtorr VCH and 96-mtorr oxetane) to 174 mtorr (approximately 30% yield over the 500 pulses). By using the same initial ratio of Ox1 to VCH, but a higher power, 0.68 J, some butadiene was observed along with the EVE and biacetyl. In this case, the amount of butadiene was approximately 1% of the amount of EVE.

IRMP-Induced Emission. Single-pulse irradiation of 100-mtorr samples of Ox1 at frequencies known to induce decomposition also produced detectable luminescence. Figure 2 shows typical time-resolved signals resulting from irradiation of 100-mtorr Ox1 by a single pulse at a frequency of 969.16 cm^{-1}. Three characteristics of the signals were measured: peak intensity, spectral distribution, and temporal profile. The results of the emission

(15) Danen, W. C.; Jang, J. C. "Laser-Induced Chemical Processes"; Steinfeld, J. I., Ed.; Plenum: New York, 1981, pp 45–164.
(16) Tsang, W. *Int. J. Chem. Kinet.* **1970**, *2*, 311.
(17) Farneth, W. E.; Thomsen, M. W.; Schultz, N. L.; Davies, M. A. *J. Am. Chem. Soc.* **1981**, *103*, 4001.
(18) Letokhov, V. S.; Moore, C. G. In "Chemical and Biochemical Applications of Lasers"; Moore, C. G.; Ed.; Academic Press: New York, 1977; Vol 3, pp 1–165.

Table II. Reaction Efficiencies and Emission Intensities at Three Frequencies of Irradiation

freq, cm^{-1}	$(k_{rxn}$ $(cm^{-1}))/$ $(k_{rxn}$ $(969\ cm^{-1}))$	(int $(cm^{-1}))/$ (int $(969\ cm^{-1})$)
931	<0.01	0.02
969	1.00	1.00
1023	<0.01	<0.01

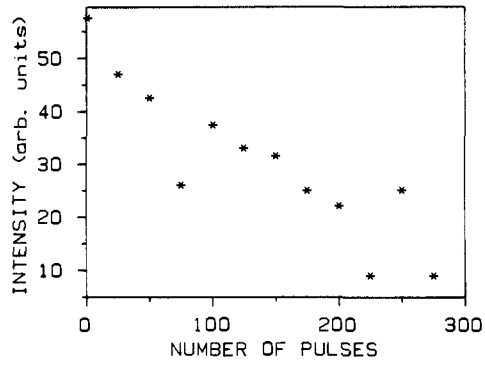

Figure 3. Peak emission intensity every 25th pulse during IR photolysis of 100 mtorr of Ox1. Data have purposely not been corrected for pulse-to-pulse fluence variations in laser output in order to show the influence of this variable.

experiments are reports of the signal in terms of these three properties. In order to compare signals following the variation of some parameter, it was necessary to reduce signal properties to meaningful quantitative values. Whether the properties of interest were intensities or decay rates, the most reliable information was obtained when these quantities were examined on a relative rather than an absolute basis.

Signal strengths were measured as peak intensities rather than integrated intensities.[19] In some cases, peak intensities could also be complicated by the presence of an initial spike which, while not entirely an artifact, was irregular in intensity. The initial spike in the signal from the PMT was due in part, but not entirely, to sparking at the windows of the cell. The fast rise of the spike portion of the signals was indistinguishable in time from signals observed when empty cells were irradiated. *All* signals disappeared when the beam was blocked from entering the enclosure or when the shutter to the PMT was closed. Unless otherwise stated, the results reported refer to intensities taken following at least a 2-μs delay from the laser pulse.

The relative peak intensities of the unresolved emission at three different frequencies of irradiation are compared with the relative IRMP-induced k_{rxn} in Table II. The intensities are the average of several single pulses at equivalent fluence. As this data suggest, significant luminescence is observed only when decomposition occurs, and the intensity of the luminescence is correlated with the extent of reaction (compare Figure 1). Furthermore, the luminescence intensity, like the decomposition yield, is strongly dependent on the laser pulse energy (Table I). The intensity of signals following IRMP irradiation of Ox2 were much smaller than that observed with Ox1 or Ox3. At powers that gave per pulse yields comparable to Ox1, the signals from Ox2 were at least a factor of 10 smaller.

Figure 3 shows the intensity (peak) of single-pulse signals every 25th laser pulse during a 275-pulse photolysis of Ox1. The intensity of the signal decreased as the number of pulses delivered to the sample increased.[20] The data over the first 200 pulses can be described by a first-order decay whose rate constant is 3.6×10^{-3} $pulse^{-1}$. This compares well with the rate constant obtained from following the pressure rise ($k_{rxn} = 1.4 \times 10^{-3}$ $pulse^{-1}$). The

(19) This assumes that the shape of the intensity profile did not vary with the parameter being changed. This treatment generally appears to be adequate. Trends with peak intensity reproduce trends with integrated intensity where the comparison has been made.

(20) The principal cause of deviations from monotonic behavior could be shown to be pulse-to-pulse variations in laser power.

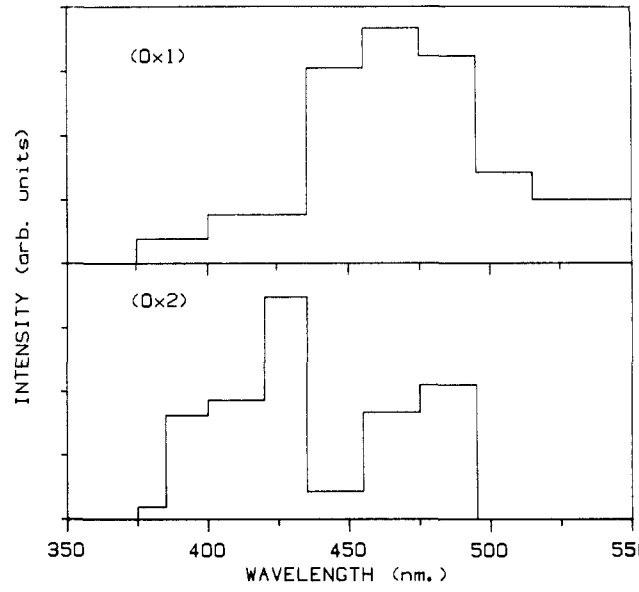

Figure 4. Reconstructed emission spectra from Ox1 (upper) and Ox2 (lower).

Table III. Effect of Bath Gases on Peak Intensities and Signal Fall-Times ($1/k_d$)

bath gas press. mtorr	peak int. of emisn		$1/k_d$ μs	
	O_2	N_2	O_2	N_2
0	168	168	13.6	13.6
250	71	62	11.1	11.2
500	18	27	8.7	9.6
750	15		9.2	
1000		6		9.1

difference between the two values can be reduced by using the integrated areas rather than peak intensities to measure the signal strength.

The spectral distribution of the emission was characterized by measuring the intensity change observed when the wavelength of long-pass cut-off filters placed in front of the PMT was gradaully increased. With each filter the intensity was normalized to the intensity observed when a 375-nm filter was used. The difference in normalized intensities between two successive filters, divided by the separation of the cut-off wavelengths of the two filters, yields an average intensity for the region defined. The intensity calculated for a certain window was multiplied by the average PMT sensitivity through that region of the spectrum. This corrected value was then plotted against the wavelength to give the coarse-grained-spectrum of the emission following irradiation of Ox1 that is shown in Figure 4. The emission detected following the IR irradiation of Ox2 was treated in the same way. The reconstructed emission spectrum for Ox2 is also shown in Figure 4. The spectral constitution of the emissions from these two oxetanes is drastically different. Note that while almost none of the signal following irradiation of Ox1 was filtered by a 435-nm cut-off filter, the same filter removed some 70% of the emission resulting from irradiation of Ox2. The spectral properties of the emission from irradiation of Ox3 were not characterized.

The fraction of the Ox2 total emission signal collected at wavelengths greater than 495 nm was determined from the ratio of the intensity passed by the 495-nm filter to the intensity passed by the 375-nm filter. The fractional contribution of the "red" (>495 nm) emission was determined under various conditions. Variation of both fluence (Table I) and bath-gas pressures (Table III) had a major impact on the total emission but a negligible influence on the "red" contribution. Within a single pulse experiment, however, the relative contribution of the long wavelength emission was found to vary with time delay from the laser pulse. For example, at 100 mtorr, the "red" fraction had values of 0.25 $\pm$ 0.05 at the peak ($\sim$4 μs) and 0.38 $\pm$ 0.05 at 15 μs.

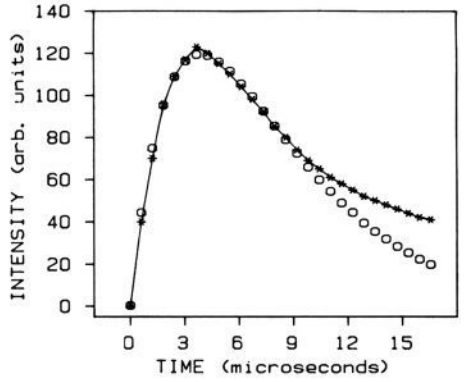

Figure 5. Emission from a single pulse of 100 mtorr of Ox1 (initial spike deleted) is shown (*) along with a fit to eq 1 (O) (vide infra).

While an appropriate temporal description of the signals was the most difficult quantity to deal with, there were certain characteristics typical of all signals. The rise of the signal from the PMT was approximately simultaneous with the laser pulse. In some instances a small incubation period was present. Accurate estimates of the incubation period were usually obscured by the spike portion of the signal. The signal decayed with a half-life of 2–15 μs.

Reduction of the $I(t)$ data to rate constants by using various fitting procedures was attempted. No simple function that was adequate over the entire time domain was identified. The first 10 μs could often be adequately fit by a single exponential rise and a single exponential fall, i.e., $I(t)=C[\exp(-k_r t) - \exp(-k_f t)]$. Figure 5 shows a typical fit with $k_r^{-1} = 3.7$ μs and $k_f^{-1} = 4.0$ μs. However, the deviation beyond 10 μs is already apparent, and the deviation becomes increasingly severe at longer times. The emission decay is multiexponential.

For purposes of comparison, we have chosen to characterize the decay as the best fit to a single exponential of data taken between 12 and 55 μs after the laser pulse (k_d). k_d increased regularly from 5.8×10^4–6.8×10^4 s^{-1} between fluences of 1.70 and 2.21 J/cm^2. Values of k_d as a function of bath-gas pressure are shown in Tables III. k_d shows a small increase with an increase in bath-gas pressure. N_2 and O_2 are indistinguishable in their effect on k_d.

Experiments were also run to determine whether the size and shape of the cell would significantly effect the temporal behavior of the signal. Decay times were measured from signals obtained in experiments using cells of three different internal diameters varying over a range of 1.5. No variation in the decay rate constants was detected for experiments of similar conditions but different cell dimensions.

Discussion

The reactivity of these oxetanes, particularly the predominant reaction along the lowest energy-thermal pathway, and the variation in yields with experimental parameters are typical of what has come to be expected of large molecules at relatively low pressures in IR photochemistry.[15,17,22] Very similar behavior with respect to fluence variation, frequency dependence, "temperature-probe molecules", and bath-gas quenching has been documented previously on other systems.[15,17,22,23-27] From these parallel observations, the now well-established model for this chemistry seems clearly applicable.[22,28] As applied to this experiment the model may be summarized briefly as follows: Vibrationally-excited oxetane molecules are prepared during the laser pulse by sequential multiphoton absorption of laser radiation. Unimolecular reaction occurs during the laser pulse in competition with further up-pumping and following the laser pusle in competition with collisional quenching. Experimental variables, like fluence, frequency, and pressure affect the magnitude of these energy-acquisition and energy-loss rates and, thereby, influence yields and product distributions. Statistical theories are entirely adequate for modeling reaction-rate constants within this framework.[22,23]

The average energy of decomposing molecules, $\bar{E}$, can be determined by comparing estimates of the energy-dependent unimolecular rate constant, $k(\bar{E})$, with values calculated from statistical theories over a range of internal energies. Values of $k(\bar{E})$ have been obtained in various ways; from chemical branching ratios,[29,30] for example, or by elegant dynamical methods.[31,32] For the limited purposes of this discussion, an order of magnitude estimate of $k(\bar{E})$ can be made by considering the restrictions placed on $k(E)$ by the pressure, laser intensity, and vibrational-state densities in these experiments. During the laser pulse, the average reacting molecule cannot reach energies above that where the rate of reaction equals the rate of up-pumping. We may estimate that the rate constant for up-pumping is given by $k_{up} = \sigma_{10} I$ where σ_{10} is the cross section for absorption of the first photon and I is the laser intensity.[15] This value would be $\sim 10^7$ s^{-1} for our system, and constitutes an upper limit to $k(\bar{E})$. Most chemistry, however, probably occurs after the laser pulse. Following the laser pulse, collisional deactivation sets a lower limit of $\sim 10^5$ s^{-1} on $k(\bar{E})$.[33] Therefore, we expect that $k(\bar{E})$ is of the order of 10^6 s^{-1} in these experiments. RRKM calculations for Ox1 give $E = 110$ kcal/mol for $k(\bar{E}) \simeq 10^6$ s^{-1}.[7]

The IRMP-induced decompositions of Ox1–3 are very clean. The two major products from each oxetane are a carbonyl portion (biacetyl, acetone, and biacetyl) and an enol–ether portion (EVE, EVE, and 2-methoxypropene). No evidence was found for either formaldehyde or the enol ethers which would result from the fragmentation along the other set of ring bonds. This preference for one reaction pathway over another has been observed in the thermal decomposition of several oxetanes.[34] Estimates[35] of the heats of formation of the most stable biradicals along each of the two reaction paths show them to differ by about 4 kcal/mol in favor the fragmentation mode that is observed experimentally. Assuming that this 4 kcal/mol can be used to represent the difference in threshold energies between the preferred and alternative fragmentation pathways and that the A factors for each pathway are equivalent, RRK calculations predict a branching ratio of >15 at $E = 110$ kcal/mol. Since the branching ratio should be larger at lower energies, the absence of products from the alternative retro-cycloaddition channel can be rationalized within the framework of the semiquantitative model described above.

All three oxetane decompositions are relatively free of products that could be ascribed to secondary reactions. The most likely secondary reaction (in the cases of Ox1 and Ox3) would be the decomposition of ethyl vinyl either (EVE) to acetaldehyde and ethylene. Since this reaction has a relatively low barrier, 44 kcal/mol,[36] some EVE might be formed with adequate excess

(21) Because of the experimental difficulties in characterizing the incubation behavior, most data were taken over longer time domains that did not resolve the very early signal.

(22) King, D. S. In "Dynamics of the Excited State"; Lawly, K. P., Ed; John Wiley and Sons: New York, 1982; pp 105–189.
(23) Farneth, W. E.; Thomsen, M. W. *J. Phys. Chem.* **1983**, *87*, 3207.
(24) Buechele J. L.; Weitz, E.; Lewis, F. D. *J. Chem. Phys.* **1982**, *72*, 3500.
(25) Setser, D. W.; Nguyen, H. H.; Danen, W. *J. Phys. Chem.* **1983**, *87*, 408.
(26) Schulz, P. A.; Sudbo, Aa.; Krajnovich, D. J.; Kwok, H. S.; Shen, Y. R.; Lee, Y. T. *Annu. Rev. Phys. Chem.* **1979**, *30*, 379.
(27) Golden, D. M.; Rossi, M. J.; Baldwin, A. C.; Barker, J. R. *Acc. Chem. Res.* **1981**, *14*, 56.
(28) Quack, M. J. *Ber. Bunsen Ges. Phys. Chem.* **1979**, *83*, 757.
(29) Farneth, W. E.; Thomsen, M. W. *J. Am. Chem. Soc.* **1983**, *105*, 1843.
(30) Papagiannakopoulos, P. J.; Kosnik, K. Benson, S. W. *Int. J. Chem. Kinet.* **1982**, *14*, 327.
(31) King, D. S.; Stephenson, J. C. *J. Am. Chem. Soc.* **1978**, *100*, 7151.
(32) von Hellfeld, A.; Feldmann, D.; Welge, K. H.; Fournier, A. P. *Opt. Commun.* **1979**, *30*, 193.
(33) Assuming strong collisions, an oxetane collision diameter of 8 Å, and uniform excitation within the irradiated zone.
(34) Jones, G., II; Schwartz, S. B.; Marton, M. T. *J. Chem. Soc. Chem. Commun.* **1973**, 374.
(35) Based on group additivity values from Benson, S. W.; "Thermochemical Kinetics" 2nd ed; Wiley: New York, 1976.
(36) Blades, A. T.; Murphy, G. W. *J. Am. Chem. Soc.* **1952**, *74*, 1039.

internal energy to decompose during the same pulse in which it is formed.

However, if secondary decomposition of EVE were to be observed, EVE must be formed with a considerable amount of internal energy, enough excess internal energy for reaction rates to compete with collisional deactivation. The collision rate constant is approximately 10^6 s^{-1} under the experimental conditions. RRK calculations suggest that EVE would require an internal energy of 75 kcal/mol to have a unimolecular rate constant of 10^5 s^{-1}. The decomposition of the oxetane is essentially thermo-neutral.[35] Assuming the energy from Ox1 is distributed statistically into the oscillators of EVE and biacetyl, Ox1 would have to have had an initial internal energy of about 150 kcal/mol to yield an EVE product this hot. It is unlikely that many Ox1 molecules have this much internal energy. An $E^* > 120$ kcal/mol would be expected to show detectable amounts of both ring-cleavage reaction pathways. Hence, it is not surprising that no significant secondary decomposition of EVE is observed.

Subsequent discussion will focus on the following questions: (1) What is the origin of the luminescence? (2) How does the luminescent chemistry fit into the semiquantitative picture of the IRMP process? While the observation of luminescence following IRMP excitation is interesting, it is not, in and of itself, unique. The literature contains many instances of IRMP-induced emission.[2-5,37,38] Several mechanisms have been proposed whereby energy initially introduced into a polyatomic system as IR photons can be converted to an emitted photon in the visible range.[39-41] Whatever processes are responsible for producing the emission observed in these oxetane experiments, they must adequately account for (1) the dependence of the intensity on irradiation frequency, (2) the loss of intensity over sequential pulses (a loss that correlates to the per pulse yield of IRMP-induced oxetane chemistry), (3) the loss of intensity with increased bath-gas pressure, (4) the observed power dependence of the intensity, (5) the reconstructed emission spectra of Ox1 and Ox2, and (6) the temporal profile of the luminescence.

Possible emitters are the following: (1) the oxetanes, (2) electronically-excited closed-shell primary products of oxetane IR photolysis, (3) electronically-excited open-shell IR photolysis products (primary), (4) electronically-excited secondary products of oxetane decomposition, or (5) an electronically-excited impurity. These possibilities will be considered in the following paragraphs. It will be argued that the emitter is a closed-shell primary product of oxetane IRMP photolysis.

For Ox1-3 to be the emitter the oxetane molecule must convert vibrational energy obtained from the absorption of IR photons into disposable electronic energy. Although this process, IER (inverse electronic relaxation),[42] is consistent with some of the experimental results, there are convincing reasons to rule it out. The wavelength of emission from Ox1 should be typical of an n $\rightarrow \pi^*$ transition of an alkyl-substituted carbonyl system. Using acetone as the model one would expect the emission to have a maximum in the region of 410 nm. The lack of any appreciable emission to the blue of 450 nm following IR irradiation of Ox1 suggests that the oxetane itself is not the immediate source of the emission. Similarly for Ox2, which has no carbonyl chromophore, an emission maximum above 400 nm, as observed, would not be likely.

A priori consideration of the structure of substituted oxetanes and the energetics of reactions available to them make these molecules unlikely candidates for IER for three reasons. First, IER is a very inefficient process which, in literature examples, requires fluences more than ten times the fluences employed in these experiments.[43] Second, IER has only been observed in molecules where the energy of the excited-electronic state which is accessed is at least as low as the barrier to the lowest reaction channel. This is necessary to make IER competitive with unimolecular decomposition. Third, the ratio of state densities (excited surface to ground surface), near the origin of the excited state, is very small for these substituted oxetanes. Ox1 is estimated to have a ratio of about 10^{-23}. Other factors being equal, the efficiency of IER is believed to be a function of this ratio. Reported examples of IER to date involve small molecules (3-6 atoms) where this ratio is relatively large. State-density ratios have been calculated to be about 10^{-5} for F_2CO[43] and 10^{-7} for $CrCl_2O_2$.[44] Since the process can be thought of as a partitioning between states on two surfaces at a given energy, the smaller the ratio of state densities the less likely that the surface with the smaller state density will have significant population. This dependence on state-density ratios is not the only factor governing reverse internal conversion. It does, however, serve as an indicator for how efficient the process is likely to be if all other factors are similar.

The possibility that the emission observed in these experiments is due to an impurity must be considered because of the low intensity of the signal and the relatively high sensitivity of the detection apparatus. In all cases the oxetane samples used were purified by gas chromatography to >99.5% purity in the liquid phase. In the case of Ox1 the less than 0.5% impurity was primarily biacetyl and ethyl vinyl ether. Direct irradiation of biacetyl under experimental conditions produces no luminescence. In fact, it has been reported that IRMP excitation of biacetyl gives no luminescence even during high power, focused irradiation.[45] Ethyl vinyl ether likewise shows no emission when irradiated at the frequencies used for Ox1 decomposition. It is improbable that any other impurity, present in less than 0.5% would be the emitter. If it were pumped directly, it would have to show the same reaction tendencies as Ox1 with respect to frequency of irradiation and per pulse consumption. If it were excited by energy transfer, there would have to be another impurity, with appropriately different behavior, present in the samples of Ox2 and Ox3.

The most commonly proposed mechanism for IRMP-induced chemiluminescence is the recombination of open-shell fragments. Such species can be formed following intense IR irradiation.[46] However, it seems very unlikely that excited diatomic and triatomic fragments are being formed in these experiments. First, no products of radical chemistry are observed. Second, the unfocused beams used to effect oxetane dissociation are very mild (<3 J/cm^2) relative to the focused beams (30-150 J/cm^2) needed in general to produce open-shell fragments.[39,46] In addition, for the oxetanes, the energy barrier to formation of radical fragments should be much higher than the molecular dissociation channels. IRMP excitation is most likely to lead to open-shell products when no lower energy reaction channels to closed-shell products exist. Common fragments such as C_2*[38] and C_3*[47] can be eliminated, based on emission spectra, as possible emitters in the case of Ox1. C_2* can also be ruled out in the case of Ox2. There is no doubt, based on the reconstructed emission spectra, that the emitting species from Ox1 is different from that of Ox2. This difference also rules out fragments that should be common to both oxetanes, i.e., ·OEt, $:CH_2$, or acyl radicals.

Having eliminated the oxetane, unidentified impurities, and small fragments as likely emitting species, only the primary reaction products remain as logical candidates. Since the intensity of the emission decreases with an increasing number of pulses,

(37) Isenor, N. R.; Merchant, V.; Hallsworth, R. S.; Richardson, M. C. *Can. J. Phys.* **1973**, *51*, 128.
(38) Duignan, M. T.; Grunwald, E.; Speiser, S. *J. Phys. Chem.* **1983**, *87*, 4387.
(39) Levy, M. R.; Reisler, H.; Mangir, M. S.; Wittig, C. *Opt. Eng.* **1980**, *19*, 29.
(40) Ruhman, S.; Anner, O.; Haas, Y. *J. Phys. Chem.* **1984**, *88*, 6397 and references therein.
(41) Wolk, G. L.; Weston, R. E.; Flynn, G. W. *J. Chem. Phys.* **1980**, *73*, 1649.
(42) Karny, Z.; Gupla, A.; Zare, R. N.; Lin, T. S.; Nieman, J.; Ronn, A. M. *Chem. Phys.* **1979**, *37*, 15.
(43) Hudgens, J. W.; Durant, J. L.; Bogan, D. J.; Covaleskie, R. A. *J. Chem. Phys.* **1979**, *70*, 5906.
(44) Nieman, J.; Ronn, A. N. *Opt. Eng.* **1980**, *19*, 39.
(45) Burak, I.; Quelly, T. J.; Steinfeld, J. I. *J. Chem. Phys.* **1979**, *70*, 334.
(46) Hall, J. H.; Lesiecki, M. L.; Guillory, W. A. *J. Chem. Phys.* **1978**, *68*, 2247.
(47) Becker, K. H.; Tatarczyk, T.; Radic-Peric, J. *Chem. Phys. Lett.* **1972**, *60*, 502.

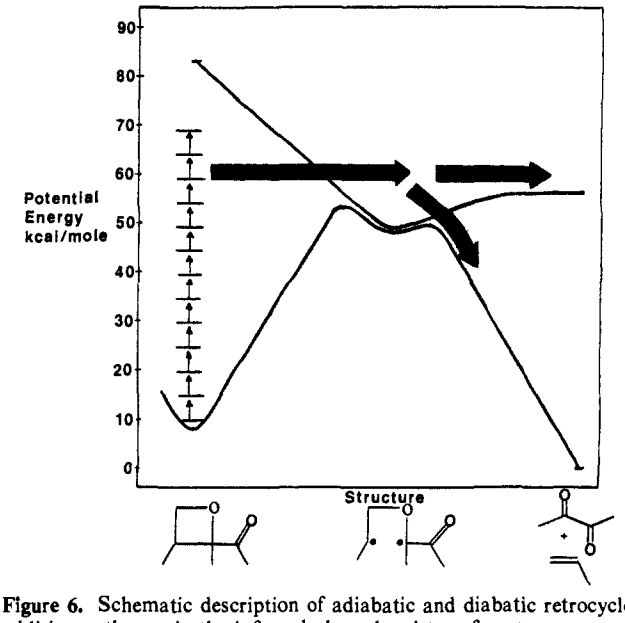

Figure 6. Schematic description of adiabatic and diabatic retrocycloaddition pathways in the infrared photochemistry of oxetanes.

it is not possible for a product molecule of one pulse to be the ultimate (or penultimate) source of the emission in a later pulse. Vibrational energy of the oxetane must be partitioned into electronic energy of the products *during* the fragmentation process. The picture that emerges from these considerations is decomposition of "hot" oxetane along competitive diabatic and adiabatic channels to a single set of products (Figure 6). The diabatic channel leads to electronically-excited ketone. In the case of Ox1, biacetyl emission apparently occurs from both the singlet and triplet manifold. The emission spectrum from Ox1 shows a maximum at 475 nm and a strong shoulder above 495 nm. Photoexcited biacetyl has emission maxima at 460 nm (singlet) and 520 nm (triplet).[48,49] By contrast, EVE, the other principal product, does not emit in this range. Similarly, the luminescence from Ox2 is consistent with emission from excited acetone. In the discussion that follows, the temporal and spectral properties of the luminescence from Ox1 will be considered in light of the known photophysics of excited biacetyl.

To a first approximation, the photophysics of electronically excited biacetyl at low pressure can be understood as a competition between emission from singlet and triplet manifolds which are essentially in equilibrium.[50] In direct photoexcitation of biacetyl, the singlet state is prepared. It decays rapidly, mainly by intersystem crossing but with some competing fluorescence. This emission has been referred by Van der Werf and Kommandeur[50] as "fast fluorescence". The lifetime of the thermalized singlet biacetyl has been determined as ~10 ns.

At low pressure, intersystem crossing tends to concentrate excited-state population in the triplet manifold because phosphorescence is slow and the reverse $T_1 \rightarrow S_1$ process is endothermic. There are low energy triplet vibronic states that cannot take part in the $S_1 \rightleftarrows T_1$ equilibrium because they do not have sufficient vibrational energy. At long times, all the excited-state population has reached these low lying triplet vibronic states. Luminescence from these states is referred to in ref 50 as "slow phosphorescence". The thermalized triplet has a lifetime of ~1.8 ms.

Between the very fast fluorescence and the very slow phosphorescence lies a median time domain, where the relaxation kinetics is quite complex. Van der Werf and Kommandeur describe a "slow fluorescence" and a "fast phosphorescence" that exhibit the same decay times and are differentiated only by the wavelength of emission. Luminescence in this median time domain effectively monitors the population of excited biacetyls residing in the triplet manifold with energies of excess of the S, T gap (~2000 cm^{-1}). The zero-pressure decay from these states is very energy dependent and varies from 45 to 0.2 μs at energies from ~3000 to ~6600 cm^{-1} above the triplet origin. These lifetimes are also sensitive to pressure and were observed to be ~5 μs and 0.15 μs, respectively, at a higher pressure, 100 mtorr of biacetyl.

The luminescence observed following IRMP-induced decomposition of Ox1 is consistent with the emission characteristics of photoexcited biacetyl in the intermediate time domain. It shows wavelength distributions that suggest both singlet and triplet emitters ("slow fluorescence" + "fast phosphorescence"), time constants that are sensitive to fluence and pressure, and multiexponential decays in the 10^4–10^6 s^{-1} range. In the direct photoexcitation experiments this time domain maps excited biacetyl at intermediate stages of relaxation with modest amounts of vibrational energy. If excited-state biacetyl is being formed from the IRMP-induced decomposition of Ox1, it almost certainly carries some internal vibrational energy as well. The average reacting oxetane molecule contains on the order of ~110 kcal/mol of energy to be partitioned at fragmentation (vide infra). If 57 kcal/mol are required to form the triplet, then ~53 kcal/mol remain to be divided among the degrees of freedom of the two products. While the overall picture is much too complex to analyze quantitatively, the general features of the model seem perfectly adequate as a rationalization of our observations.

A basic kinetic scheme (Scheme I) that represents this model would be the following:

Scheme I

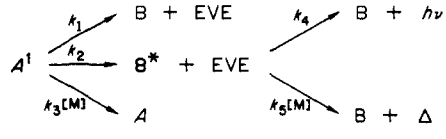

A^1 represents the population of vibrationally-excited oxetane molecules present at the termination of the laser pulse. These molecules may react via k_1 to ground-state products or via k_2 to excited-state products, or they may be relaxed by collisions. B* represents the population of excited biacetyl molecules. k_4 represents luminescent decay channels of that population. The luminescence intensity, I, monitors the population of B^* (eq 1) where

$$I \propto [B^*] = C(e^{-k_r t} - e^{-k_f t}) \qquad (1)$$

k_r contains all the terms that lead to decay of A^1 and k_f contains all the terms that lead to decay of B^*. Previous discussion suggests that both k_r and k_f are probably dominated by collision-induced vibrational relaxation. This would make them similar in magnitude in the 10^5–10^6 range. Indeed, our best attempts to fit the early-time data to an equation of the form of eq 1 yields $k_r = 2.8 \times 10^5$ s^{-1} and $k_f = 2.5 \times 10^5$ s^{-1}, as shown in Figure 5. The decay time constants become longer, and the spectrum red-shifts at longer delay times as collisions cause the population in the low-lying triplet levels to grow. As these low-lying levels are populated, the slow phosphorescence plays an increasingly prominent role in the luminescence. Following Scheme I, increased fluence increases decay rates because B^* is formed with somewhat more energy. At higher energies, biacetyl radiative lifetimes are shorter and luminescence plays a larger role in k_f. Similarly, increased pressure increases decay rates because the collisional relaxation rates that contribute to k_f, that is, k_5[M] in Scheme I, are directly proportional to pressure.

Our best estimate of the partitioning between adiabatic and diabatic channels suggests a ratio of $k_2/k_1 \leq 10^{-4}$. However, this calculation is very sensitive to luminescence quantum yields which the Van der Werf and Kommandeur data show are strongly dependent on vibrational energy and pressure. Because the energy distributions in these experiments are so poorly defined, this partitioning ratio should be considered no better than an order of magnitude approximation.

We are inclined to view luminescence from Ox2 and Ox3 in similar terms. Chemiluminescence from Ox2 is clearly different

(48) Reference 9 and reference therein.
(49) Parmenter, C. S.; Poland, H. M. *J. Chem. Phys.* **1969**, *51*, 1551.
(50) van der Werf, R.; Kommandeur, J. *J. Chem. Phys.* **1976**, *16*, 125.

from both Ox1 and Ox3 and is spectrally consistent with acetone. The significantly lower intensity from Ox2 could be the result of (1) the higher excited-state energies of acetone leading to poorer competition of the diabatic channel with adiabatic reaction or (2) the lower luminescence quantum yields of acetone or both. To the extent that we have characterized its luminescence, Ox3 behaves like Ox1, as would be expected from their common fragmentation products.

Photochemical Implications. Many photochemical systems are thermally reversible. Some oxetanes thermally revert to the ketone and olefin[51] from which they were photochemically formed. Any process by which a molecule breaks down to give the chemical species from which it was formed is obviously the "reverse" (chemical) of the formation reaction. So in that limited sense, the thermal chemistry of oxetanes can be considered the reverse of photochemical cycloaddition. However, a careful analysis of the reaction mechanism reveals that the photocycloaddition is fundamentally different from the thermal decomposition. There are, for example, many different ways in which excess energy could be partitioned in proceeding from the oxetane to a carbonyl and an olefin. Since the formation of oxetanes by the Paterno–Buchi reaction is diabatic, only those decomposition pathways along which energy partitoning leads to an excited-state carbonyl can be considered the formal reverse. That is, the dissociation of an oxetane is the formal reverse of the Paterno–Buchi reaction if and only if the same (two) energy surfaces are involved in both the formation and dissociation of the oxetane—but traversed in opposite order.

The formal reverse of any diabatic photochemical reaction is difficult to obtain. There are no other reported examples where a diabatic photochemical reaction has been formally reversed.[52] Since forward diabatic photochemical reactions return a molecule to the ground-state surface with significant excess vibrational energy, the formal reverse reaction pathway requires the initial production of a highly vibrationally-excited ground-state molecule. IRMP excitation is an ideal method for effecting the instant heating required to access these high-lying vibrational states.

The ability of IRMP excitation to promote otherwise minor or unobservable higher energy pathways has been demonstrated in numerous IRMP photolyses where both competing pathways are ground state (adiabatic) channels. Because up-pumping is faster than reaction until well above the critical energy, the reacting molecules usually have significant amounts of excess internal energy. For example, IRMP excitation of vinyl cyclopropane leads to average internal energies of reacting molecules some 25 kcal/mol above the lowest energy reaction channel.[17]

Consequently, reaction channels not prominent during normal pyrolysis compete. The observation we have made, in the oxetane system, that the higher energy channel can be a diabatic version of the principal reaction pathway is an interesting variation on this phenomenon.

While the behavior of these selected oxetanes is unique, we feel it has an additional significance. By establishing a pair of diabatic reactions, one the formal reverse of the other, one presents a system (and more broadly a methodology) for studying surface crossings from either direction. By altering the substituent pattern on the oxetane it will be possible to examine the effects of heavy atoms and radical stabilizing substituents on the efficiency of surface crossing. Preliminary experiments addressing the role of a biradical intermediate in the reverse of the Paterno–Buchi reaction have been executed. We believe that the IRMP methodology for studying diabatic chemistry introduced here promises to be a useful tool in mechanistic photochemistry.

Acknowledgment. We are grateful for the support of this work by the Department of Energy, Office of Basic Energy Sciences.

(51) Jones, G. *Org. Photochem.* **1981**, *5*, chapter 1.
(52) Turro, N. J.; Chow, M. *J. Am. Chem. Soc.* **1979**, *101*, 1300 is a related example.

Complexes of Macrocyclic Polyethers and Neutral Guest Molecules: A Systematic Approach to the Complexation of Water Molecules by 2,6-Pyridinium Crown Ethers[1]

Peter D. J. Grootenhuis,[†] Jos W. H. M. Uiterwijk,[§] David N. Reinhoudt,*[†] Catherina J. van Staveren,[†] Ernst J. R. Sudhölter,[†] Martinus Bos,[‡] Johan van Eerden,[§] Wim T. Klooster,[§] Laminus Kruise,[§] and Sybolt Harkema[§]

Contribution from the Laboratories of Organic Chemistry, Chemical Analysis, and Chemical Physics, Twente University of Technology, 7500 AE Enschede, The Netherlands.
Received July 17, 1985

Abstract: pK_a determinations of 2,6-pyridinium crown ethers **1** (n = 0–6) in four different solvent systems show that the acidity of these ligands strongly depends on ring size and solvent composition. This dependence is explained in terms of a stabilizing, macroring-assisted solvation of the pyridinium moiety, which varies with the ring size. X-ray analyses of the solid complexes of 2,6-pyrido-18-crown-6·H_2O·$HClO_4$ (1:1:1), 2,6-pyrido-18-crown-6·H_2O·HPic (1:1:1), 2,6-pyrido-21-crown-7·H_2O·$HClO_4$ (1:1:1), and 2,6-pyrido-24-crown-8·H_2O·$HClO_4$ (1:2:1) support this interpretation. The 18-membered pyrido crown ether has a structure which is optimally suited to form an encapsulated complex with water. The effect of complexation on the conformation of the macroring was studied by performing an X-ray analysis of the free 2,6-pyrido-18-crown-6. Approximate stability constants of the water complexes in the various solvent systems could be estimated from the pK_a data.

The ability of macrocyclic polyethers ("crown ethers") to form well-defined stoichiometric complexes with a variety of small, cationic guests has received much attention during the last 2 decades. Although a number of complexes between crown ethers and *neutral* molecules are known,[2] our understanding of this type

[†] Organic Chemistry.
[‡] Chemical Analysis.
[§] Chemical Physics.

(1) Part of this work appeared in preliminary form: Grootenhuis, P. D. J.; van Staveren, C. J.; den Hertog, H. J., Jr.; Reinhoudt, D. N.; Bos, M.; Uiterwijk, J. W. H. M.; Kruise, L.; Harkema, S. *J. Chem. Soc., Chem. Commun.* **1984**, 1412–1413.

0002-7863/86/1508-0780$01.50/0